

TOUGHNESS COMPARISON BETWEEN THE REHEATED INTERCRITICAL ZONE OF TWO HSLA STEELS

C.L. DAVIS and J.E. KING

*Department of Materials Science and Metallurgy
University of Cambridge, Cambridge, CB2 3QZ, United Kingdom*

ABSTRACT

High strength low alloy steels have been shown to suffer from the existence of regions of poor impact toughness within the heat affected zone (HAZ). One of these regions is the reheated intercritical zone formed during multipass welding. During the weld thermal cycles the material is initially heated to around 1350°C producing the coarse grained HAZ and then reheated into the austenite/ferrite two phase field by the subsequent pass. In this paper reheated intercritical zone microstructures and toughness have been studied for two steels, produced by different process routes, one having been reheated, quenched and tempered (RQT) after hot rolling whereas the other was direct quenched and tempered (DQT). The difference in process route allows the second steel to have a lower carbon content and carbon equivalent whilst maintaining the required mechanical properties.

KEYWORDS

HSLA steel; RQT/DQT; HAZ; reheated intercritical zone; MA constituent; LBZ; impact toughness.

INTRODUCTION

The demand for high strength, high toughness and good weldability in structural steels has prompted much research into the processing route and the plate chemistry of these steels. A reheat, quench and temper process (RQT) has been used in conjunction with controlled rolling or thermal mechanical controlled processes (TCMP) to produce steels of guaranteed quality. A further enhancement in the quest for high quality steels is the new direct quench process (DQ) pioneered by the Japanese [Heedman and Sjostrom (1982); Bessyo et al. (1984); Watanabe et al. (1986)]. Here the steel is quenched immediately after hot rolling and the required mechanical properties are obtained by a subsequent temper. It is also possible to reduce the carbon content and the carbon equivalent of the steel whilst maintaining its mechanical properties with careful microalloying additions when using this route. Another advantage is the increase in production efficiency due to the elimination of the reheat during processing.

The high strength and toughness balance achieved by these processing routes may be disturbed by the thermal cycles received during welding producing areas of poor toughness known as local brittle zones (LBZ's). One of these areas found in the heat affected zone (HAZ) of many high strength low alloy (HSLA) steels is the reheated intercritical zone formed by the effect of two welding passes [Kim et al. (1991); Haze et al. (1987); Akselsen et al. (1987); Suzuki et al. (1989)]. This zone is formed when the initial coarse grained region, generated on experiencing a peak temperature of about 1350°C adjacent to the first weld bead, is reheated to about 750°C by the influence of the second weld bead.

This paper investigates the toughness of the reheated intercritical zone of two HSLA steels (referred to as the intercritical zone), one produced by the RQT process and the other by the DQT process, with particular reference to their microstructures.

MATERIALS AND MICROSTRUCTURE

The composition of the steels used is given in table 1

Table 1. Chemical composition of the steels used (weight %).

	C	Si	Mn	Cr	Mo	Ni	Nb	Ti	V
Steel 1	0.09	0.30	1.25	0.12	0.12	0.50	-	0.05	0.01
Steel 2	0.048	0.30	1.22	0.06	0.05	0.50	0.015	0.012	0.05

Both steels were hot rolled to 25mm plate. Steel 1 was air cooled, reheated into the austenite region, quenched and tempered resulting in a fine grained microstructure composed of ferrite with areas of tempered bainite/martensite, figure 1a). Steel 2 was quenched directly after rolling and subsequently tempered giving a similar microstructure to that seen for steel 1 except for the smaller amount of bainite/martensite areas because of the lower carbon content, figure 1b). The mechanical properties of the steels are similar, because of their similar microstructures, and both show good toughness, strength and hardness.

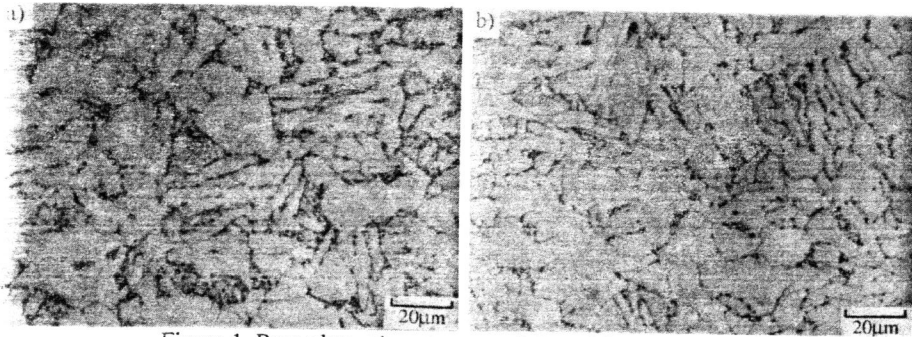


Figure 1. Base plate microstructure of a) steel 1 and b) steel 2.

EXPERIMENTAL TECHNIQUES

Due to the narrow, discontinuous nature of the local brittle zones of interest in-situ testing within the HAZ after welding is difficult. Consequently a Smitweld thermal cycle simulator was used to reproduce the microstructures of interest allowing close control of the critical parameters. For the thermal simulations the parameters controlling the first cycle were kept constant, peak temperature of 1350°C and a cool time between 800 and 500°C of 30 seconds, whilst the peak temperature of the second thermal cycle (T_{p2}) was varied between 650 and 850°C with a constant effective cool time.*

Specimens measuring 10x10x55mm were simulated producing, a region of uniform microstructure measuring 10x10x7mm suitable for Charpy V notch testing. The fracture surfaces were examined in an SEM and a number of samples were nickel plated and sectioned perpendicular to the fracture surface and the region below the surface studied metallographically. The microstructures were etched using LePera etchant (a 1:1 mixture of 1% aqueous solution of

* For a T_{p2} of less than 800°C a cool time is calculated to give a cooling curve identical to that obtained when 30 seconds is used between 800 and 500°C.

sodium metabisulphite and 4% picral) [LePera (1979)]. Microhardness measurements using a 100g load were made on each microstructure.

RESULTS AND DISCUSSION

Coarse Grained HAZ Formed During a Single Cycle Simulation. The coarse grained microstructures for steels 1 and 2 are shown in figure 2a) and b) respectively. For steel 1 the microstructure consists of coarse upper bainite with large prior austenite grain size due to the high degree of grain growth that occurs on heating to 1350°C. This microstructure is common for many HSLA steels of similar composition [Haze et al. (1987); Koo and Ozekcin (1987); Krishnadev et al. (1987)]. However steel 2 shows a predominantly fine grained ferritic structure with some areas of upper bainite. This results from its lower carbon content (and carbon equivalent) and possibly a degree of grain boundary pinning by microalloy carbides (niobium and vanadium).

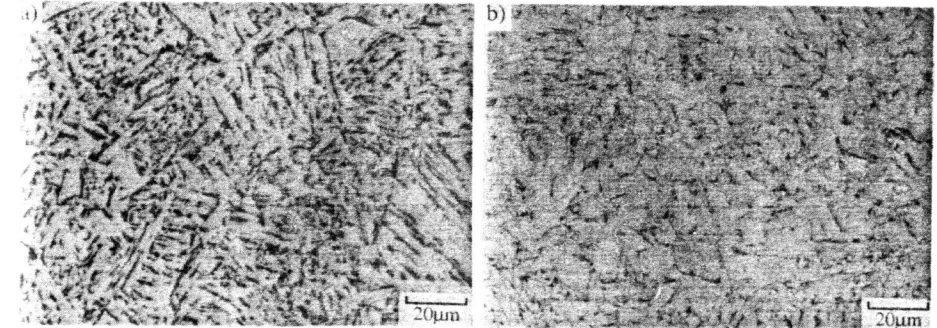


Figure 2. Coarse grained HAZ microstructure for a) steel 1 and b) steel 2.

Second Cycle Simulations. Examining the Charpy impact energy as a function of the second cycle peak temperature (T_{p2}) for both steel 1 and steel 2, figure 3a), it can be seen that there is a marked reduction in toughness at T_{p2} of about 770°C for steel 1, the intercritical zone. Figure 3b) shows the microhardness data over the range of T_{p2} values indicating that the loss of toughness seen for steel 1 and the toughness difference between the two steels is not due to any strength differences. The full ductile-to-brittle transition curves of the base plate, the coarse grained HAZ (formed after a single cycle of peak temperature of 1350°C) and the intercritical zone for steels 1 and 2 are shown in figure 4a) and b) respectively. Figure 4a) shows the shift in the ductile brittle transition temperature (DBTT) of the intercritical zone to higher temperature emphasising its poor toughness, whereas in figure 4b) the DBTT's of all three structures are very similar indicating that there is only a slight deterioration in toughness for the intercritical zone.

The microstructures of steel 1 for second cycle peak temperatures of 720°C, 780°C and 830°C, figure 5a)-c), show that at 720°C, the *subcritical zone*, the microstructure consists of a tempered coarse upper bainite, i.e. a tempered coarse grained HAZ structure, figure 5a). The tempering results in the high toughness seen for this structure. At T_{p2} of 830°C the material is just heated into the austenite field and on cooling multiple ferrite nucleation occurs resulting in the *fine grained zone* microstructure which gives good toughness, figure 5b). The *intercritical zone* formed in the T_{p2} range of 760-790°C has a distinctive microstructure formed when the initial coarse grained structure is heated into the austenite/ferrite two phase field, figure 5c). During the second cycle austenite preferentially nucleates and grows along the prior austenite grain boundaries. These austenite islands become carbon enriched and on cooling transform to give a hard and brittle product, they also give the structure its characteristic 'necklace' appearance. SEM analysis of this grain boundary product reveals the nature of this phase which has been identified as MA constituent (high carbon martensite with some retained austenite) in figure 6a) and as part

MA and part upper bainite or fine pearlite in figure 6b) [Ikawa et al. (1980); Lanzillotto and Pickering (1982)].

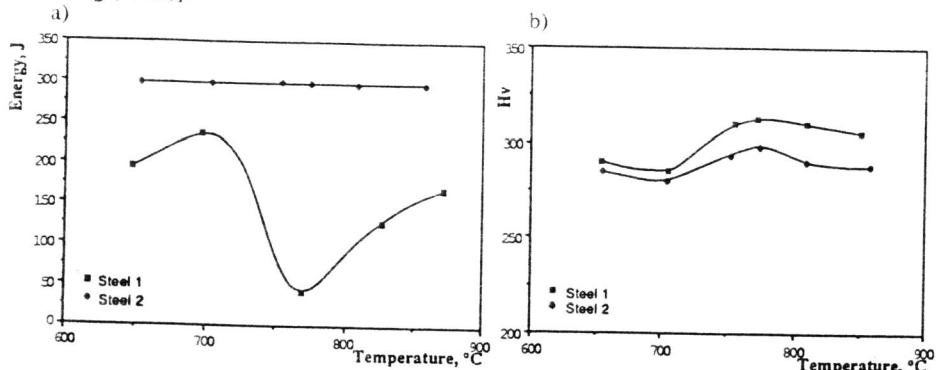


Figure 3. a) Charpy impact toughness and b) microhardness as a function of second cycle peak temperature for steels 1 and 2.

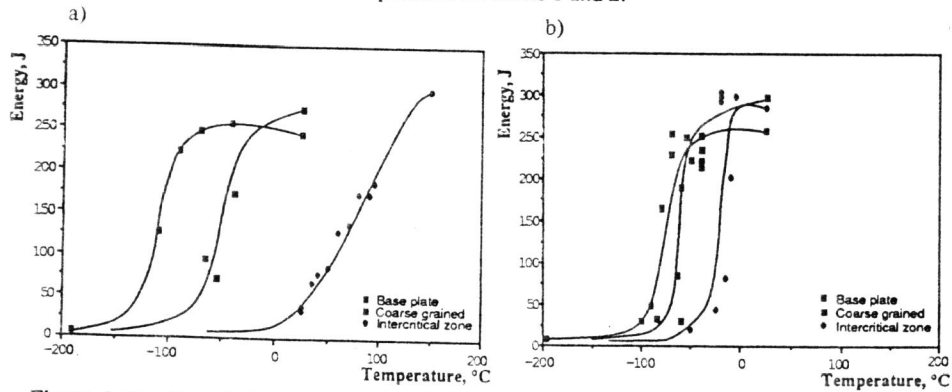


Figure 4. Ductile to brittle transition curves for the base plate, the coarse grained HAZ and the intercritical zone for a) steel 1 and b) steel 2.

For steel 2 the microstructures over the range of T_{p2} values have a similar fine grained appearance to that seen for the initial 'coarse grained' HAZ microstructure, although for T_{p2} values above about 780°C there are no areas of upper bainite seen, figure 7. This explains the good toughness seen over the range of T_{p2} values. However Charpy testing at -50°C indicates a reduction in toughness above T_{p2} of 750°C, figure 8. Closer examination of the microstructures in the SEM reveals a difference in the structure of the dark areas seen optically. Above T_{p2} of 750°C these areas are predominantly MA constituent, figure 9a), whereas below 750°C these areas are tempered martensite/ferrite and carbides, figure 9b). The MA constituent is seen because heating above 750°C allows the carbon rich areas in the original microstructure to transform to austenite and on cooling these areas then give MA, whereas below 750°C the original carbon rich areas are tempered.

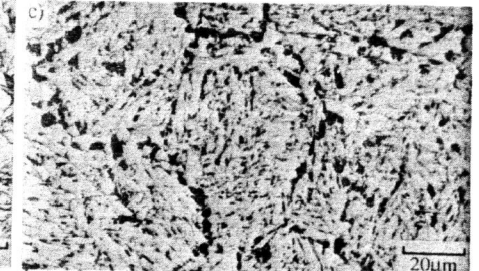
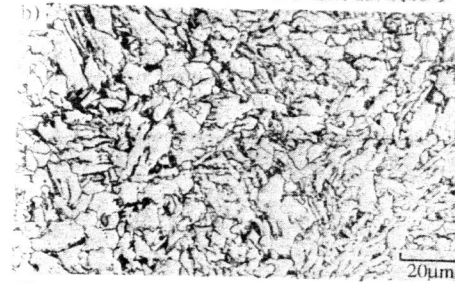
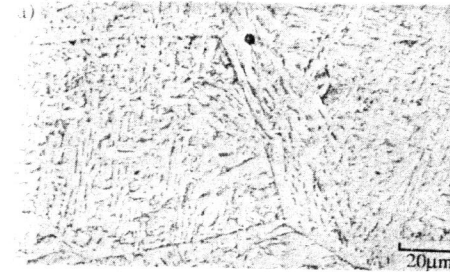


Figure 5. a) T_{p2} 720°C, subcritical zone, b) T_{p2} 830°C, fine grained zone, and c) T_{p2} 780°C, intercritical zone, for steel 1.

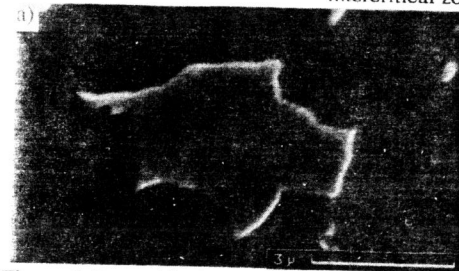


Figure 6. Intercritical zone grain boundary microstructure showing a) MA constituent and b) part MA part upper bainite/ fine pearlite for steel 1.

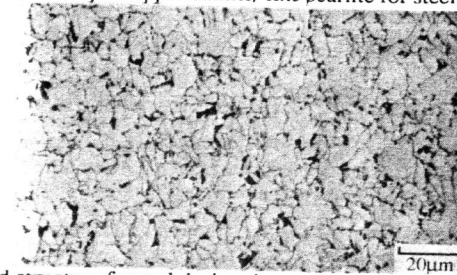


Figure 7. Fine grained structure formed during the second thermal cycle above 780°C for steel 2.

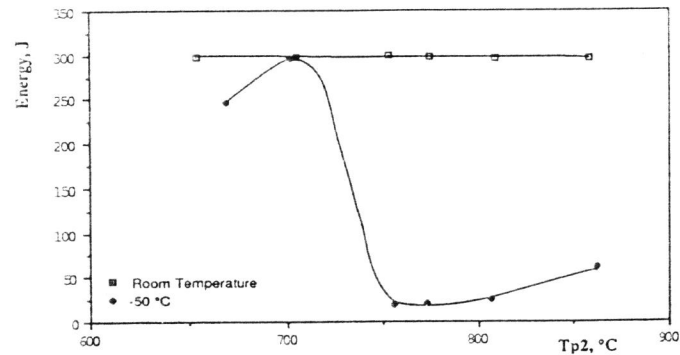


Figure 8. Charpy impact toughness as a function of T_{p2} for steel 2 at room temperature and -50°C .

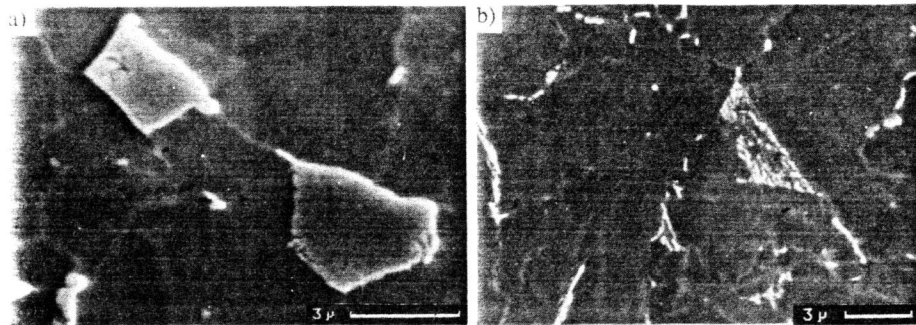


Figure 9. Intercritical zone microstructure showing a) MA constituent and b) tempered martensite/ferrite and carbides for steel 2.

The reason for the low toughness of the intercritical zone of steel 1 is associated with the presence of a connected/near connected grain boundary phase of fully or part MA constituent and has been described in detail by the authors elsewhere [Davis and King (1992)]. In brief the main reason is that the MA particles at the grain boundary debond and interact to cause a local stress concentration which can result in a microcrack forming. This acts as an initiation site for failure by transgranular cleavage, figure 10.

In the case of steel 2 the MA constituent is still present but no longer as a connected/near connected grain boundary phase. Fractographic studies show that the MA phase still debonds from the matrix, figure 11, but no longer causes local failure. Reduction in toughness on Charpy testing at -50°C for values of T_{p2} above 750°C shows that the presence of MA phase is detrimental to the toughness but not to the extent seen for steel 1. The reason for this appears to be that the MA phase does not belong to a connected/near connected network. Hence on debonding there is no interaction between particles but there is some degree of stress concentration, accounting for the reduction in toughness observed at low temperatures.

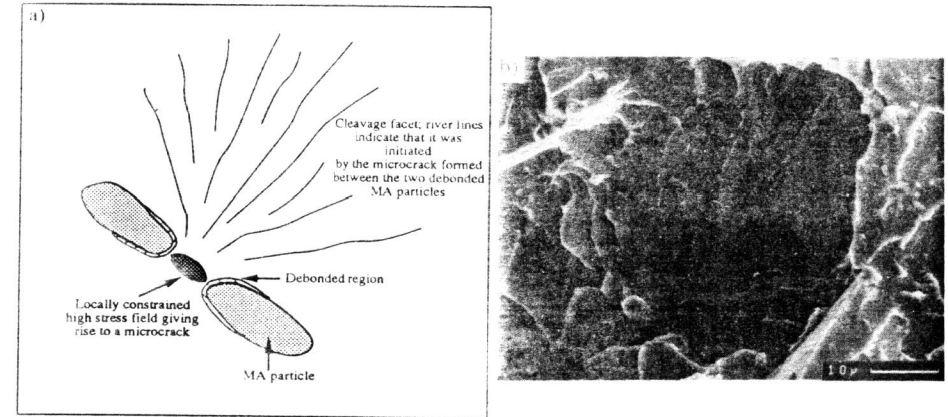


Figure 10. a) Schematic diagram and b) an actual cleavage facet showing the proposed mechanism by which the connected/near connected MA particles initiate cleavage.



Figure 11. Matching cleavage facets for steel 2 showing a debanded MA particle.

CONCLUSIONS

Weld simulation samples were used to investigate the microstructure and toughness of the intercritical zone of two HSLA steels with similar strength levels but different compositions, one formed by the reheat, quench and temper process (RQT) and the other by the direct quench and temper process (DQT). The main conclusions are as follows.

1. Steel 1 shows a marked reduction in toughness for the intercritical zone formed for a second cycle peak temperature of $760\text{--}790^{\circ}\text{C}$. The loss in toughness is associated with the formation of a connected/near connected grain boundary phase of fully or part MA constituent.
2. Steel 2 does not show any reduction in toughness after intercritical heating for Charpy testing at room temperature due to its fine grained structure. However toughness is reduced for values of

Tp₂ above 750°C, shown by Charpy testing at -50°C. This is associated with the formation of MA constituent.

3. Fractographic studies reveal that the MA particles debond from the matrix for the intercritical zone of both steels. However a connected/near connected grain boundary phase of MA constituent is required for a marked loss of toughness.

ACKNOWLEDGEMENTS

The financial support of the Science and Engineering Research Council and British Steel plc, is gratefully acknowledged. The material was provided by British Steel, Swinden Laboratories. Thanks are also due to Professor C.J. Humphreys for the provision of research facilities at Cambridge.

REFERENCES

- O.M.Akselsen, Ø.Grong and J.K.Solberg. Structure-property relationships in intercritical heat affected zone of low carbon microalloyed steels. *Mat. Sci. and Tech.* **3** Aug 1987, 649-655
- K.Bessyo, H.Koshinaga, S.Watanabe, M.Nakamura and S.Suzuki. Manufacture of heavy plate by applying direct quenching. *Tetsu-to-Hagane* **70** (10), 1984, 93-99
- C.L.Davis and J.E.King. The effect of cooling rate on intercritical zone microstructure and toughness in a HSLA steel. To be published, *Mat. Sci. and Tech.* 1992
- T.Haze, S.Aihara and H.Mabuchi. Characteristics of high-strength steel plates for low temperature service with high weldability and HAZ toughness imparted by controlled rolling and accelerated cooling. *Proc. or the Int. Symp. of Acc. Cooling of Rolled Steel.* 1987, 235-247
- P.Heedman and A.Sjostrom. Direct quenching of controlled rolled C-Mn steel plates. *Scand. J. Metallurgy.* **11**, 1982, 233-238
- H.Ikawa, H.Oshige and T.Tanoue. Effect of martensite-austenite constituent on HAZ toughness of a high strength steel. *Trans. of the Japan Welding Soc.* **11** (2), Oct 1980, 3-12
- B.C.Kim, S.Lee, N.J.Kim and D.Y.Lee. Microstructure and local brittle zone phenomena in high-strength low alloy steel welds. *Met. Trans A.* **22A**, Jan 1991, 139-149
- J.Y.Koo and A.Ozekcin. Local brittle zone microstructures and toughness in structural steel weldments. *Met. Soc. Int. Symp. on Welding Met. of Structural Steels.* Denver, Colorado, 1987
- M.R.Krishnadev, J.T.McGrath, J.T.Bowker and S.Dionne. HAZ microstructure and toughness of precipitation strengthened HSLA steels and conventional HY-Grade high strength steels. *Welding Met. of Structural Steels.* Ed. J.Y.Koo, Pub. AIME TMS, 1987, 137-155
- C.A.N.Lanzillotto and F.B.Pickering. Structure-property relationships in dual phase steels. *Met. Sci.* **16** Aug 1982, 371-383
- F.S.LePera. Improved etching technique for the determination of percentage martensite in high strength dual phase steels. *Metallography.* **12** 1979, 263-268
- S.Suzuki, K.Arimochi, J.Furusawa, K.Bessyo and R.Someya. Development of LBZ-free low Al-B treated steel plate. *The Eighth Int. Conf. on Offshore Mechanics and Arctic Engineering.* The Hague, March 1989, 657-663
- S.Watanabe, K.Arimochi, N.Komatsubara, H.Yoshinaga and S.Suzuki. Development of high strength steel plate with superior weldability by direct quenching process. *The Sumitome Search.* **32** May 1986, 42-52